Adv. Polar Upper Atmos. Res., 16, 111-125, 2002


# Polar mesosphere winter echoes during solar proton events

S. Kirkwood[1], V. Barabash[1], E. Belova[1], H. Nilsson[1], T.N. Rao[1], K. Stebel[1], A. Osepian[2] and Phillip B. Chilson[3]

[1]*Swedish Institute of Space Physics, Box 812, 981 28 Kiruna, Sweden*
[2]*Polar Geophysical Institute, Halturina 15, Murmansk, Russia*
[3]*Cooperative Institute for Research in Environmental Science (CIRES) University of Colorado, Boulder, CO, U.S.A.*

***Abstract***: Thin layers of enhanced radar echoes in the winter mesosphere have been observed by the ESRAD 52 MHz MST radar (67°53′N, 21°06′E) during several recent solar proton events. These polar mesosphere winter echoes (PMWE) can occur at any time of day or night above 70 km altitude, whereas below this height they are seen only during daytime. An energy deposition/ion-chemical model is used to calculate electron and ion densities from the observed proton fluxes. It is found that PMWE occurrence correlates well with low values of $\lambda$ (the ratio of negative ion density to electron density). There is a sharp cut-off in PMWE occurrence at $\lambda \sim 10^2$, which is independent of electron density. No direct dependence of PMWE occurrence on electron density can be found within the range represented by the solar proton events, with PMWE being observed at all levels of electron density corresponding to values of $\lambda < 10^2$. Together with results concerning the thickness, echo aspect-sensitivity and echo spectral-width of the PMWE, this observation leads to the conclusion that the layers cannot be explained by turbulence alone. A role for charged aerosols in creating PMWE is proposed.

## 1. Introduction

VHF radar echoes from the high-latitude mesosphere are well known to be much weaker in winter than in summer. The first studies using the powerful Poker Flat radar in Alaska (location 65.12°N, 147.43°W, with transmitter power 2 MW, and antenna area 40000 m$^2$) were reported by Ecklund and Balsley, 1981 and Balsley *et al*., 1983. Wintertime echoes were seen between 50 and 80 km and reached levels 30 dB lower than summertime echoes, which were concentrated at heights 80–90 km. The strong summertime layers between 80–90 km have since been termed 'Polar Mesosphere Summer Echoes', or PMSE, and have been detected and studied by several radars around the world. They are today thought to be caused by the effects of layers of small charged aerosols on the radar refractive index (see *e.g*. Cho and Röttger, 1997 for a review). Regarding the winter echoes, on the other hand, Balsley *et al*. (1983) noted that they appeared to be correlated with high-energy particle precipitation enhancing the ionization in the mesosphere, and that vertical profiles of echo power were highly structured on scales of 5–15 km. The echoes were interpreted as due to turbulence caused by breaking gravity waves. Note, however, that the limited height resolution of the Poker Flat radar (2.2 km) precluded

study of the structure on smaller scales, and no systematic study was made of the echo dependence on ionisation levels in the surrounding atmosphere. Wintertime echoes at high latitudes have been further studied by Czechowsky *et al.* (1989), using the SOUSY mobile radar during a campaign from Andöya, northern Norway in 1983/84 (location 69.17°N, 16.01°E). Results similar to those from Poker Flat were found and it was confirmed that the echoes were detectable only during periods when electron densities were enhanced by energetic particle precipitation. It was noted that enhanced electron densities during the hours of darkness seemed not to lead to observable echoing layers below about 70 km altitude. Also in this case, the echoing structures were said to have vertical extent of 2–10 km. Although the SOUSY radar operated with high resolution (300 m or better) and examples of layers as narrow as the resolution can be found in the figures in Czechowsky *et al.* (1989), no comment was made on the thinness of the layers and turbulence due to wave saturation and/or breaking was again proposed as the cause.

In this paper we examine the characteristics of mesospheric winter echoes using the ESRAD MST radar located at Esrange, near Kiruna in Sweden (67.88°N, 21.10°E). A detailed description of the radar can be found in Chilson *et al.*, 1999. This radar uses 72 kW transmitter power and a 1600 $m^2$ antenna array, together giving about 30 dB (1000 times) less sensitivity than the Poker Flat or SOUSY mobile radars. ESRAD is normally used to study Polar Mesosphere Summer Echoes (*e.g.* Kirkwood *et al.*, 1998) and tropospheric winds and waves (*e.g.* Réchou *et al.*, 1999). However it operates continuously, monitoring also wintertime radar returns from the stratosphere and mesosphere. During the winter 2000/2001 several solar proton events occurred and during these events mesospheric layers were detected by the ESRAD radar. We refer to these layers as Polar Mesosphere Winter Echoes (PMWE). The good height resolution and detailed analysis available with the ESRAD spaced-antenna configuration (see *e.g.* Holdsworth and Reid, 1995) allow new characteristics of the layers to be determined. Because of the long duration of the solar proton events (several days) and the availability of satellite data on the precipitating protons, we are able to model realistically the electron density variations in the mesosphere during both day and night conditions. This allows us to separate electron density dependence from solar illumination dependence. Together, these analyses lead to new interpretations of the cause of PMWE.

## 2. Characteristics of PMWE

Radar returns from the height region 5–100 km are monitored routinely by the ESRAD radar with 600 m height resolution and time resolution varying from one profile each 7 min to 1 profile every third minute. For the second half of the winter 2000/2001, the region 60–80 km was also monitored with 300 m resolution. (1 profile each 3 min). Examples showing the most intense layers detected in November and April are shown in the panels second from the top in Figs. 1 and 2a, respectively. The colour scales for the plots have been chosen so that the highest tops in the background noise are just visible (blue). The noise can be seen as a generally randomly placed pixels, although sometimes forming vertical lines due to interfence reaching the receivers. The PMWE appear as layers of enhanced radar echo power above this noise level—generally green, yellow or red in the plots. The layer thicknesses (FWHM) are, at times, as little as, or less than, the

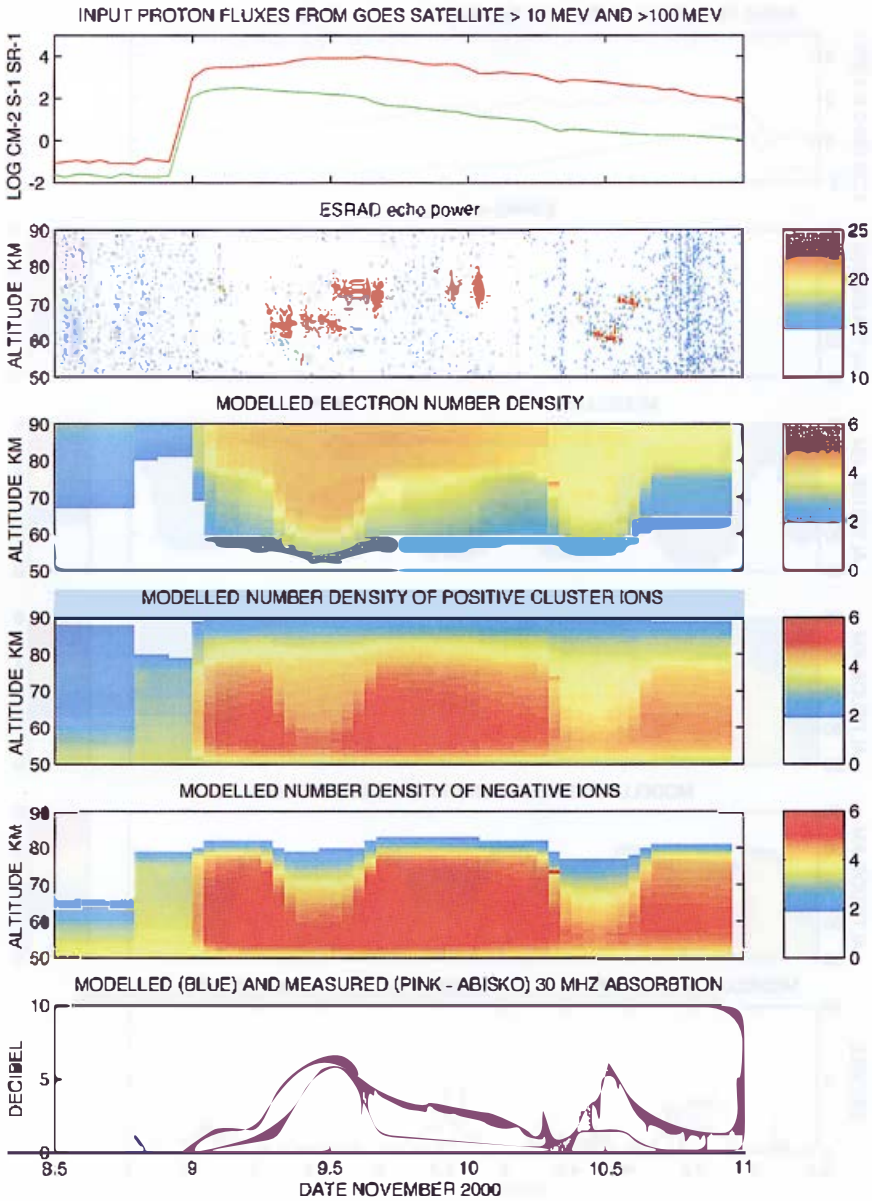


*Fig. 1. Observations and model results for 9–10 November 2000. The x-axis shows the date and time (UT) as a decimal fraction of the day (e.g. '9.5' for 12 UT on 9 November). Top panel: Solar proton fluxes from GOES 10 satellite. 2nd panel: Echo power recorded by the ESRAD radar (colour scale dB). 3rd–5th panels: Modelled densities of electrons, positive cluster ions and negative ions. Colour scale shows log density $cm^{-3}$. 6th panel: Cosmic noise absorption at 30 MHz calculated from the model results (blue) and measured (magenta) by a riometer in Abisko, 80 km WNW from ESRAD.*

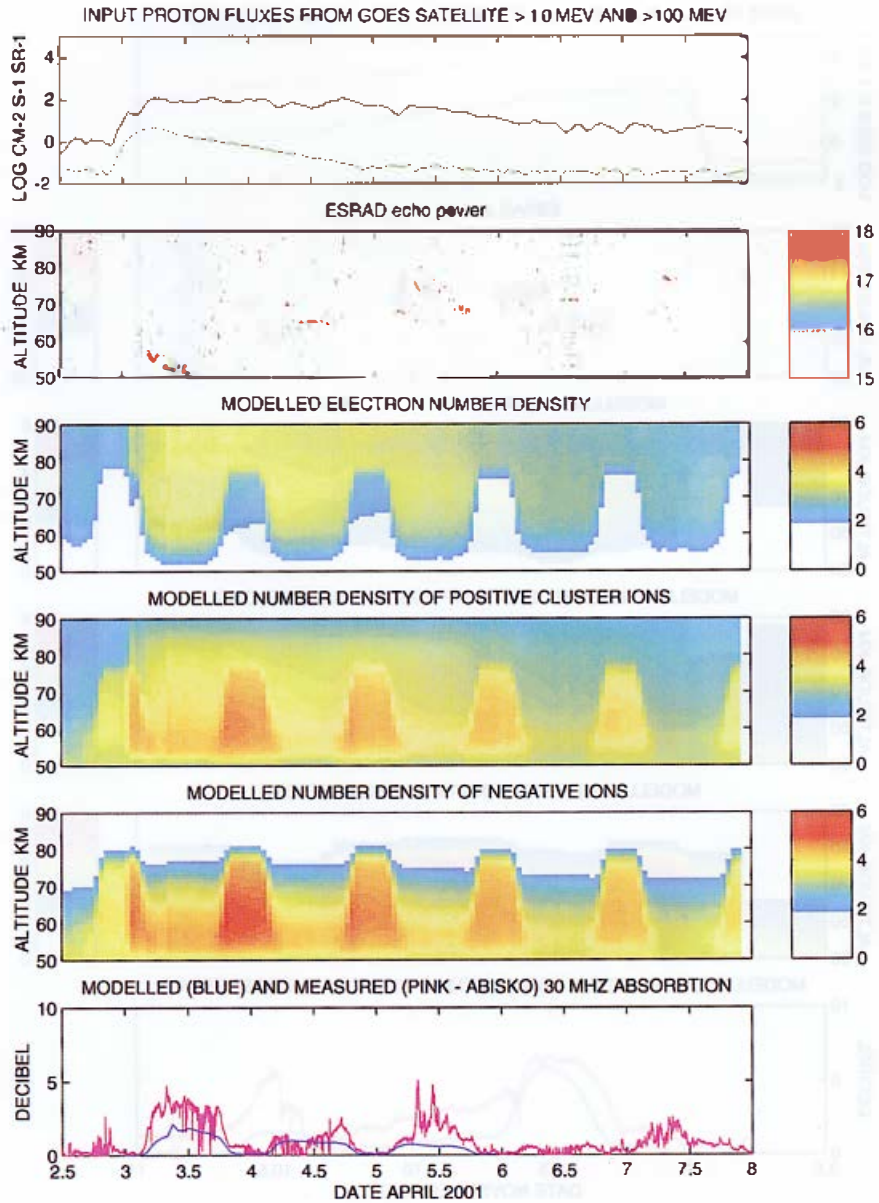


*Fig. 2a. Observations and model results for 2–7 April 2001. The x-axis shows the date and time (UT) as a decimal fraction of the day (e.g. '3.5' for 12 UT on 3 April). Top panel: Solar proton fluxes from GOES satellite. 2nd panel: Echo power recorded by the ESRAD radar (colour scale dB). 3rd–5th panels: Modelled densities of electrons, positive cluster ions and negative ions. Colour scale shows log density $cm^{-3}$. 6th panel: Cosmic noise absorption at 30 MHz calculated from the model results (blue) and measured (magenta) by a riometer in Abisko, 80 km WNW from ESRAD.*

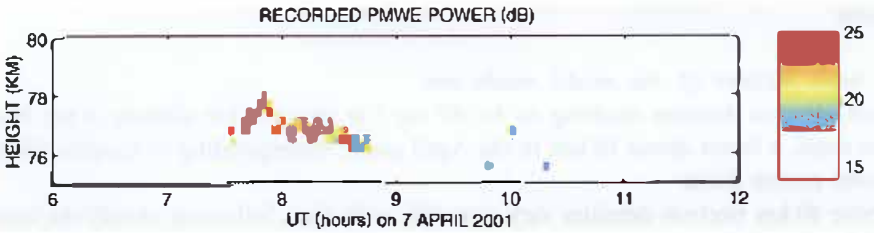


*Fig. 2b. Enlargement showing the < 300 m thick PMWE seen on 7 April 2001.*

resolution of the observations, particularly for the layers seen in April (Fig. 2a). The PMWE are easy to identify in Fig. 1 where they are rather broad in height and generally last several hours at a time They are less easy to identify in Fig. 2a where they are generally much narrower in height and more sporadic in time. However, careful inspection shows identifiable layers each day, in the midday sector—below 60 km on 3 April, close to 65 km on 4 April, 70 km on 5 April, just above 70 km on 6 April and at about 77 km on 7 April. This last layer, on 7 April, is almost impossible to see in Fig. 2a because of its extreme thinness. It is shown in enlargement in Fig. 2b. Note that the resolution on this day was 300 m and the PMWE for most of the time occupies only one range gate.

Similar layers were seen during all of the solar proton events which occurred between October 2000 and early May 2001 (in October, November, January, March, April and early May). However no layers other than the usual PMSE lying between 75–90 km were seen during the solar proton event which occurred in July 2000, despite proton fluxes 60% higher than the event in Fig 1. No layers were seen either during solar proton events in August and September 2000. This justifies the term 'winter' in the name PMWE. Layers were not seen at times other than during solar proton events. Since such events affect the mesosphere only at high latitudes, this leads to the term 'polar' in the name PMWE.

To examine the dependence of PMWE on the density of free electrons and ions in the mesosphere we have used the energy-deposition/ion-chemical model described in Kirkwood and Osepian, 1995. Tests of the model, including its application to solar proton events, can be found in the same publication. As input to the model we have used a Maxwellian flux-energy spectrum of precipitating protons fitted to the integral fluxes at $>$ 10 Mev and $>$ 100 MeV measured by the GOES 10 satellite (http://www.sec.noaa.gov/ftpmenu/lists/particle.html). The proton fluxes are shown in the top panel of Figs. 1 and 2a. Model results for the solar proton event of 9–11 November 2000 are shown in the 3rd–6th panels of Fig. 1, and for 2–7 April in Fig. 2a. The lowest panels of Figs. 1 and 2a also show the observed absorption of cosmic radio noise at 30 MHz, from the nearby riometer station of Abisko, Sweden. Comparison between this measured absorption and that calculated on the basis of the model electron density profiles gives a measure of how well our model probably represents the real situation in the atmosphere (at least concerning electron density). In general the model results predict lower absorption than observed. Similar daily variations with constant discrepancies in amount (*e.g.* up to a factor 2) are likely due to minor inadequacies in the model, *i.e.* electron densities being underestimated by up to a factor 2 at all heights, or the extension of ionisation to lower heights being underestimated in the model. Large discrepancies and/or rapid time variations in the observed absorption are likely due to precipitation of energetic electrons, in addition to the

protons.

*The main features of the model results are:*

- peak electron densities reaching *ca* $4\times10^4$ cm$^{-3}$ at about 70 km altitude in the November event, a factor about 10 less in the April event, corresponding to roughly 100 times lower proton fluxes
- above 80 km electron densities vary smoothly with time, following closely the intensity of the proton fluxes
- below 80 km electron densities have a strong daily variation. The explanation for this is to be found in the behaviour of the negative ions which are most persistent at night. This in turn is explained by the fact that electrons are readily removed from negative ions by sunlight and by reactions involving atomic oxygen, which is present in much greater amounts during daytime
- high densities of positive cluster ions below 80 km, reaching $>10^5$ cm$^{-3}$ (in November), with a strong daily variation. This daily variation is due to the reduction in recombination at night as the number of free electrons is diminished.

A comparison between the 2nd and 3rd panels of Fig. 1 or between the 2nd and 3rd panels of Fig. 2a suggests a correlation of PMWE with high densities of free electrons, with PMWE being absent below 75 km at night, *i.e.* when and where the electrons attach instead to negative ions. However, a closer comparison between Figs. 1 and 2a shows that the daytime layer on 4 April (centre of Fig. 2a) is present in a background of slightly lower electron density than that which prevails at the same height during the night of 9/10 November. This suggests that the primary parameter controlling the daily variation of PMWE during solar-proton events is not the absolute electron density but rather some effect related to the absence of negative ions (or the presence of atomic oxygen).

To gain more information concerning the dependence of PMWE on electron density or ion composition, all of the radar profiles collected between 1 September 2000 and 30 April 2001 have been searched for statistically significant features as follows: first each height profile (20–100 km with 600 m resolution) is examined and any point lying more than 3 standard-deviations above the mean is identified as a possible PMWE. Next, time continuity is tested by checking whether similarly enhanced signal is present in the following two height profiles, at the same or adjacent altitudes. Each height and time bin satisfying both criteria is recorded as containing PMWE. The detected PMWE and their temporal correspondence to solar proton events is tabulated in Table 1. Only 10% of the detected PMWE are found at times when there is no detectable increase of proton flux. They might be due to enhanced proton fluxes which we cannot detect, or to other sources of ionisation such as high-energy electron precipiation. All detected PMWE are included in Fig. 3 as it is always possible to estimate corresponding values of $\lambda$ according to the solar elevation (see below). PMWE occurring when the proton fluxes are below the detection threshold are not included in Fig. 4 since it is not possible to calculate corresponding electron densities in these cases.

Figure 3 shows the height and solar-elevation for all of the PMWE seen during the whole winter period against a background of contours of $\lambda$, the ratio of negative ion density to electron density. The dependence of on solar elevation shown in Fig. 3 has been calculated using fixed proton fluxes (values at 12 UT on 9 November). Although the

*Table 1. Dates and lengths of time when proton fluxes (> 10 MeV) were above the detection threshold for the GOES-10 satellite and characteristics of PMWE during these periods. The bottom row summarises PMWE detected when proton fluxes were below the detection threshold.*

| Dates | Total time (hours) with proton flux $>0.16$ cm$^{-2}$s$^{-1}$sr$^{-1}$ | Maximum proton flux (cm$^{-2}$s$^{-1}$sr$^{-1}$) | Total time PMWE detected (hours) | Maximum PMWE power (dB) |
|---|---|---|---|---|
| 2000 Sep 8 | 8 | 0.23 | 0 | |
| 2000 Sep 12-21 | 160 | 178.75 | 2 | 11 |
| 2000 Oct 1 | 2 | 0.16 | <1 | 10 |
| 2000 Oct 7-14 | 38 | 0.32 | 0 | |
| 2000 Oct 16-23 | 94 | 4.33 | 0 | |
| 2000 Oct 25-31 | 100 | 6.28 | 6 | 12 |
| 2000 Nov 1-6 | 39 | 2.15 | 3 | 18 |
| 2000 Nov 8-23 | 355 | 9741.66 | 25 | 22 |
| 2000 Nov 24-30 | 164 | 665.66 | 5 | 13 |
| 2000 Dec 1-8 | 96 | 1.04 | 2 | 12 |
| 2000 Dec 21 | 2 | 0.16 | <1 | 9 |
| 2000 Dec 28 31 | 30 | 0.30 | <1 | 10 |
| 2001 Jan 1-3 | 5 | 0.17 | 0 | |
| 2001 Jan 5-7 | 27 | 0.41 | <1 | 9 |
| 2001 Jan 15 16 | 9 | 0.21 | 1 | 12 |
| 2001 Jan 21 27 | 104 | 1.47 | 3 | 13 |
| 2001 Jan 28-31 | 73 | 29.07 | 1 | 12 |
| 2001 Feb 01-02 | 7 | 0.21 | 0 | |
| 2001 Feb 11 12 | 14 | 0.28 | <1 | 9 |
| 2001 Feb 18 | 2 | 0.19 | 0 | |
| 2001 Feb 25-28 | 29 | 0.67 | <1 | 9 |
| 2001 Mar 10-11 | 4 | 0.16 | <1 | 8 |
| 2001 Mar 15 17 | 5 | 0.18 | 0 | 0 |
| 2001 Mar 23 | 2 | 0.17 | <1 | 13 |
| 2001 Mar 26-28 | 32 | 1.94 | <1 | 8 |
| 2001 Mar 29-31 | 61 | 21.70 | 4 | 12 |
| 2001 Apr 1-9 | 210 | 126.16 | 7 | 19 |
| 2001 Apr 10-14 | 114 | 286.16 | 2 | 24 |
| 2001 Apr 15-17 | 70 | 341.25 | 2 | 17 |
| 2001 Apr 18-27 | 177 | 188.83 | 2 | 21 |
| 2001 Apr 28-29 | 23 | 15.35 | <1 | 13 |
| Total | 2087 | | 71 | |
| 2000 1 Sep 2001 31 April flux $<0.16$ cm$^{-2}$s$^{-1}$sr$^{-1}$ | 3721 | <0.16 | 8 | 14 |

absolute values of electron density and negative ion density may vary by orders of magnitude from one event to another, the ratio $\lambda$ is approximately constant for any particular solar-zenith elevation and height. For example, the 2-3-orders of magnitude difference in absolute electron and ion densities between 9 November in Fig. 1 and 7 April in Fig. 2a corresponds to , at most, a factor 2 change in $\lambda$. It is very clear that PMWE are seen only where $\lambda$ is low—*i.e.* above *ca* 75 km altitude at any time of day, below that height only during daytime when there is a large proportion of free electrons and a small proportion of negative ions. The only layers which do not seem to fit this pattern very well are those below 55 km altitude. However, the uncertainties in the ion-chemistry

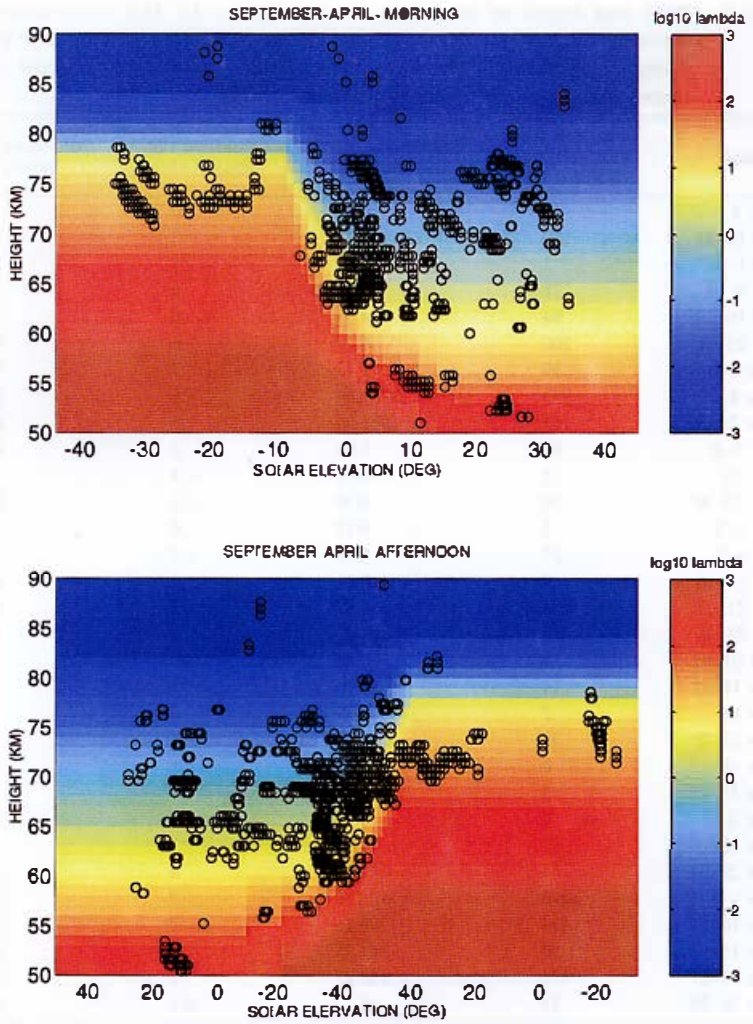


*Fig. 3. Detected PMWE as a function of height and solar elevation (deg) plotted against a background (colour) showing the corresponding log ($\lambda$), $\lambda$ being the ratio of negative ion density to electron density. The upper panel is for morning (solar elevation increasing with time), the lower panel for evening.*

model is greatest at these low heights so the apparent discrepancy may simply be an artifact of the model. Altogether, the attachment of electrons to form negative ions at night (high $\lambda$) is well correlated with an absence of PMWE.

To further try to separate the dependence on electron density from the dependence on ion composition, a model value of electron density and ion composition is calculated for each detected PMWE, using the corresponding height, solar elevation and solar proton flux. Figure 4 plots detected PMWE as a function of both model electron density and $\lambda$. Individual layers can be seen in several cases as they trace a steady reduction in electron density as $\lambda$ increases, *i.e.* as the solar elevation decreases. The number of hours of

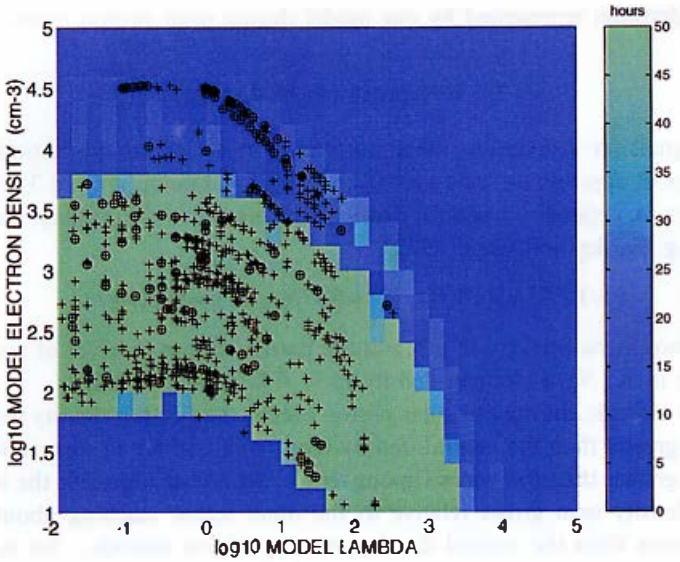


*Fig. 4. Detected PMWE as a function of model values of log (λ) (λ being the ratio of negative ion density to electron density) and log (electron density) calculated using the ion-chemistry model for the appropriate height, solar elevation and solar proton flux (+ and ●). The background (colour) shows the number of hours during which radar observations were made for the corresponding electron density/λ conditions. The dark blue areas correspond to ranges of electron density/λ for which we have no observations.*

observations for the different λ/electron density conditions are shown by the coloured background. We are able to compute model values of electron density and λ only when proton fluxes are above the detection threshold for the GOES 10 satellite (*ca* 0.16 protons $cm^{-1}\ s^{-1}\ sr^{-1}$). This means that only such conditions are represented in Fig. 4, *i.e.* there is no information on the presence or absence of PMWE for the lowest values of both electron density and λ simultaneously, since such conditions do not occur so long as proton fluxes exceed the GOES 10 detection threshold.

Two symbols are used to indicate PMWE observations: '+' show all detected layers between September 2000 and April 2001, '●' show those events where the integral 30 MHz noise absorption from the model is in such close agreement with observed values that we can be sure there is no significant extra ionisation due to precipitating high-energy electrons. In the other cases, energetic electrons from the magnetosphere must be contributing to the electron density profile. It is known from statistical studies that most of the effect from magnetospheric electrons is at heights above 90 km so it is unlikely that they have a significant effect at the heights of the observed layers (50-90 km). However it cannot be categorically ruled out. Despite this uncertainty, it is still rather clear that PMWE have a sharp cut-off as λ increases above 100 ($10^2$) even though their environment in terms of electron density can vary by several orders of magnitude at this cut-off. At low values of λ, PMWE are seen at electron densities as low as $10^2\ cm^{-3}$. At high values of λ, PMWE are not seen even though electron densities as high as $3\times10^3\ cm^{-3}$ occurred during many hours. If there is a threshold electron density required for PMWE , then it

is below the densities represented by our model during solar proton events.

## 3. Interpretation of PMWE

Radar signals are scattered by the atmosphere when there are fluctuations in the radar refractive index at appropriate scale sizes (for the ESRAD radar, around 3 m). The radar refractive index, n, depends on neutral density, temperature and humidity, and on electron density (see *e.g.* Balsley and Gage, 1980).

$$n = 1 + 77.6 \times 10^{-6}(p/T) + 0.373(e/T^2) - 40.3(Ne/f^2),$$

where $p$ is atmospheric pressure in mb, $e$ is the partial vapour pressure of water, in mb, $T$ is temperature in K, $Ne$ is electron density $m^{-3}$, $f$ is radar frequency.

At 50 km altitude, during our solar proton events, the electron density term is an order of magnitude greater than the neutral density term ($p/T$) which in turn is about 3 orders of magnitude greater than the water vapour term. At higher altitudes, the importance of the electron density term grows relative to the other terms, reaching about 5 orders of magnitude greater than the neutral density term by 80 km altitude. So to explain our PMWE we must find a mechanism which causes fluctuations in electron density along the direction of the radar beam including scale-sizes of 3 m.

Before discussing possible causes further, it is worth considering what more information about the scattering mechanism we can derive from the properties of the radar echoes. Using the spatial correlation method and the spectral widths of the radar echoes it is possible to estimate the random spread of velocities within the scattering volume (turbulence) and the anisotropy (ratio of vertical thickness to horizontal length) of the scattering structures (Holdsworth and Reid, 1995). Since rather strong signal levels are needed for such analysis, we have been able to estimate these parameters only for the strongest layers seen during our observation period. These are given in Table 2. We will return to these values in the discussion below.

The first explanation to be considered is that the layers are due to turbulence due to gravity-wave breaking or Kelvin-Helmholz instability (due to wind shear), as proposed for high-latitudes by Balsley *et al.*, 1983 and Czechowsky *et al.*, 1989. Turbulence due to enhanced gravity wave breaking at temperature inversions has also been proposed to cause layers of enhanced radar-echoes. Studies at mid- and low-latitudes (Thomas *et al.*, 1996; Ratnam *et al.*, 2002) have found a close correlation between enhanced radar echoes and strong temperature inversions seen by lidar in the 70–80 km height interval. Lübken (1997), through a succession of sounding rocket experiments, has indeed been able to demonstrate that narrow layers of strong turbulence are a common feature of the winter mesosphere. Further, in the presence of an electron density gradient, neutral turbulence would be expected to cause turbulence also in the electron plasma. However, the layers found by Lübken (1997) were generally a few km thick, much more than the $<300$ m we observe for the PMWE in Figs. 2a and 2b. The lower latitude radar-echo layers observed by Thomas *et al.* (1996) to be correlated with temperature inversions have also been rather broad (more than 2 km thick).

Typical turbulent velocities implied by the rocket experiments reported by Lübken (1997) were *ca* 1–2 $ms^{-1}$. This is close to the values we find for the relatively thick

*Table 2. Radar echo parameters for the three strongest layers observed. The rms turbulent velocity is derived from the doppler spread of the echo spectrum, the aspect sensitivity (and irregularity length/height ratio) are from spatial correlation analysis (see Holdsworth and Reid, 1995).*

| Date | 9 November 2000 | 10 November 2000 | 7 April 2001 |
|---|---|---|---|
| Time | 07-13 UT | 11-13 UT | 07-10 UT |
| Layer center height | 63-65 km | 60-62 km | 77-78 km |
| Layer thickness | <0.6-2.4 km | <0.6-1.2 km | <0.3-0.6 km |
| Height resolution | 0.6 km | 0.6 km | 0.3 km |
| Rms turbulent velocity | 1.7 m/s | 1.7 m/s | 0.2 m/s |
| Aspect sensitivity | 1.3° | 1.9° | 1.3° |
| Irregularity length/height ratio | 12 | 8 | 12 |
| Model electron density | 3000-24000 $cm^{-3}$ | 1000-3000 $cm^{-3}$ | 300-400 $cm^{-3}$ |
| Model electron density gradient | $10^{-2}$-$5\times10^{-2}$ $cm^{-4}$ | $3\times10^{-1}$-$10^{-2}$ $cm^{-4}$ | $2\times10^{-4}$-$4\times10^{-4}$ $cm^{-4}$ |

November PMWE (Fig. 1 and Table 2) but much more than we find for the very thin PMWE on 7 April 2001 (Fig. 2b and Table 2). The anisotropy we find for all of the PMWE is rather high. This indicates that, if PMWE are due to turbulence, that turbulence must be highly anisotropic. It might also indicate that the echoes are due to Fresnel reflection from multiple sharp layers rather than from turbulence. A further problem with the turbulent-layer hypothesis is the behaviour with respect to electron density. A turbulent layer should simply redistribute the background electron density with the irregularity strength directly related to electron density gradient. The electron density gradients at the relevant heights during solar proton events are, with normal ion-chemistry, directly related to the electron density itself. For constant turbulence intensity, we would expect to see PMWE getting steadily weaker as the electron density (and its gradient) decrease. We would not expect a layer with weak turbulence (7 April, rms turbulent velocity 0.2 $ms^{-1}$) to be seen at an electron density of only 400 $cm^{-3}$ (gradient $4\times10^{-4}$ $cm^{-4}$) while a layer with strong turbulence (9 November, rms turbulent velocity 1.7 $ms^{-1}$) becomes abruptly too weak to detect as soon as the electron density falls to 3000 $cm^{-3}$ (gradient $10^{-2}$ $cm^{-4}$).

However, the major problem with the turbulent-layer hypothesis arises when we consider Lübken *et al.*'s (1993) results concerning their direct observations of the inner scale of turbulence in wintertime turbulent layers. These show that the inner scale length of the turbulence (in the neutral air density) is of the order 4-12 m, so that neutral-density fluctuations start to be attenuated at the shorter scale-sizes (3 m) needed to explain the PMWE. The relationship between the scale-size cut-off in neutral density and that in electron density (to which the radar is sensitive) can be conveniently categorised by the Schmidt number, which is the ratio of kinematic viscosity to electron diffusivity (Driscoll and Kennedy, 1985). When only positive ions are present, electrons are constrained by charge balance to diffuse with the ions (ambipolar diffusion) and ions and electrons have

the same diffusivity. With ion masses close to those of the main neutral molecules in the atmosphere, fluctuations in ion and electron density will then have close to the same scale-size distribution as the neutral air density (the case of Schmidt number 1, Kelley *et al.*, 1987). However, when negative ions are present, the diffusivity of the electrons is effectively increased (Hill, 1978) and the shortest-scale fluctuations in neutral and ion densities should no longer be present in the electron density. We observe PMWE at values of $\lambda$ up to about 100. According to Hill (1978) the electron diffusivity should then be increased by a factor $(1+\lambda)$, *i.e.* close to 100. This will reduce the Schmidt number to about 0.01. According to Driscoll and Kennedy (1985) this should put the 'inner scale size' for electron-density fluctuations at about 10 times more than for neutral density fluctuations, *i.e.* 40–120 m. This is far above the 3 m to which our radar is sensitive. A similar mismatch between the inner scale of turbulent fluctuations and the scale-sizes needed to give radar echoes is found for polar mesosphere summer echoes. The only reasonable way to increase the electron Schmidt number and extend turbulence-produced electron-density fluctuations to short enough scale sizes is thought to be through the presence of heavy, charged aerosols (as reviewed by Cho and Röttger, 1997). Our observations of PMWE at times when no negative ions are present might then similarly be explained by the presence of charged aerosols which increase the Schmidt number to about 100. The disappearance of PMWE at $\lambda \sim 100$ could then be explained by the increased electron diffusivity causing a reduction of the Schmidt number to about 1, at which point the inner-scale size of the electron density fluctuations should increase to above the radar half-wavelength (3 m).

We must also consider other processes than neutral turbulence which might produce fluctuations in electron density with appropriate scale-sizes. For example, we should consider that the height profile of minor constituents of importance for the ion chemistry might be highly structured. There is indeed some evidence that the vertical profile of water vapour in the high-latitude winter mesosphere contains sharp maxima and minima (Khaplanov *et al.*, 1996). To test the effect of a thin layer of enhanced water vapour we have made calculations using the ion-chemistry model described above but with double the normal water vapour concentration in a 1-km thick layer at 62–63 km altitude. The result for the conditions of 3 April 2001 is an electron density depletion (about 20%) within the enhanced water layer. This can be understood as an increase in the ratio of positive cluster ions to positive molecular ions as cluster-ion formation is favoured by increased water vapour. Since cluster ions have shorter lifetimes against recombination with electrons, the net result is a lower electron density. The gradients bounding the electron density depletion layer could, in principle, lead to enhanced radar echoes. However, the model results show that the relative depletion ($\Delta Ne/Ne$) is slightly dependent on the ionisation rate—the electron density depletion increases to 30% (day)–40% (night) if the ionisation rate is increased by a factor 10. The percentage depletion is, if anything, slightly higher at night (high $\lambda$). The net result is a strong dependence of absolute electron-density gradient on electron density. So our observation that PMWE requires low values of $\lambda$ rather than high values of electron density, does not support this explanation either.

A further possibility to consider is that PMWE, in a similar fashion to some types of PMSE, might be due to sharp gradients in electron density caused by layers of charged aerosols. Studies of the aerosol layers by a number of sounding-rocket experiments at the

summer mesopause seem to indicate the presence of both positively and negatively charged aerosols associated with 'bite-outs' in the electron density profile, presumably due to scavenging of electrons by the aerosols (*e.g.* Croskey *et al.*, 2001; Havnes *et al.*, 2001). The sharp gradients in electron density associated with such a 'bite-out' can be an effective source of highly aspect-sensitive radar echoes. If such aerosol layers were present in the winter mesosphere they could be expected to cause similar bite-outs at those heights and times of day when electrons are the only negative charge carriers (apart from the aerosols themselves).

Once large numbers of negative ions become available, they can be captured by aerosols in a similar way to electrons. Capture rates are expected to be proportional to the number flux of the charged particles $N \times C$, where $N$ is the number density of charged particles and $C$ is their mean thermal velocity (*e.g.* Natanson, 1960). The ratio of capture rates for negative ions and electrons, $R$ , can then be expressed as:

$$R \propto \lambda C_- / C_e = \lambda (m_e / m_-)^{1/2},$$

where $m_e$ and $m_-$ are the masses of electron and negative ions, respectively.

Assuming that the main negative ions are $O_2^-$, $CO_3^-$ and $NO_3^-$, this gives

$$R \propto \lambda (0.3\text{–}0.4) \times 10^{-2}.$$

Thus $\lambda = 3 \times 10^2$, about the value we find to correspond to the cut-off for PMWE occurrence, corresponds to the situation when electrons and negative ions have equal capture rates. For higher values of $\lambda$, aerosols should preferentially scavenge negative ions leading to a negative-ion 'bite-out' rather than an electron 'bite-out'. This would not cause enhanced radar echoes since the echoes require a gradient in electron density, not a gradient in ion density. Any gradient in electron density will diffuse away rapidly due to the very high electron diffusivity in the presence of negative ions (Hill, 1978).

## 4. Conclusions

Thin layers of enhanced radar-echoes between 50–80 km altitude in the winter mesosphere have been observed by the 52 MHz ESRAD radar during solar proton events. These PMWE (polar mesosphere winter layers) are seen at a wide range of background electron densities but only when the ratio of negative ions to free electrons is expected to be less than about 100. The characteristics of PMWE lead us to conclude that aerosols are most likely involved in creating electron density fluctuations at the 3 m scale-sizes necessary to produce radar echoes, in the same way as in PMSE (polar mesosphere summer echoes).

Clearly it is not reasonable to propose that water-ice aerosols are involved in PMWE as temperatures in the winter mesosphere are much too high for water saturation. Some other type of aerosol must be proposed, such as the meteoric smoke or dust proposed by Hunten *et al.*, 1981. Unfortunately, very little is known about the charging properties of such aerosols, if indeed they really are present in the winter mesosphere. However, it is interesting to note in this context that an aerosol layer at the very unusual height of 37 km was reported by several high-latitude lidar stations in mid November 2000, (K.-H. Fricke, personal communication). The layer persisted over several weeks inside the polar vortex,

sinking to about 28 km height before it disappeared in February 2001. The height of the layer seen by the lidars is clearly rather lower than the layers we see with the radar. However, as in the case of PMSE, aerosols responsible for PMWE might well be too small to be detected by lidar but could in some cases grow large enough to be seen by such instruments, at the same time sedimenting to lower altitude.

The possibility that significant numbers of aerosols are present in the winter polar mesosphere, and that they are concentrated into layers, may have considerable significance for chemical processes in the region. Chlorine activation on polar stratospheric clouds (aerosols), which is the precursor to stratospheric ozone destruction in the polar vortex, is one example of such an effect on chemistry which might then also occur in the mesosphere. The possibility of recombination of O and $H_2$ on aerosol surfaces as a source of mesospheric water vapour, is another (Summers and Siskind, 1999).

## Acknowledgments

The ESRAD MST radar is operated jointly by Swedish Institute of Space Physics and Swedish Space Corporation, Esrange. Riometer data from Abisko were provided by Sodankylä Geophysical Institute, Finland. Software for full-correlation analysis of the ESRAD data has been developed at the University of Nebraska. This research has been funded by the Swedish Science Research Council.

The editor thanks Drs. Y. Murayama and A. P. van Eyken for their help in evaluating this paper.

## References

Balsley, B.B. and Gage, K.S. (1980): The MST radar technique: potential for middle atmosphere studies. J. Pure Appl. Geophys., **118**, 452-493.

Balsley, B.B., Ecklund, W.L. and Fritts, D.C. (1983): VHF echoes from the high-latitude mesosphere and lower thermosphere: observations and interpretations. J. Atmos. Sci., **40**, 2451-2466.

Chilson, P., Kirkwood, S. and Nilsson, A. (1999): The Esrange MST radar: a brief introduction and procedure for range validation using balloons. Radio Sci., **34**, 427-436.

Cho, J. and Röttger, J. (1997): An updated review of polar mesosphere summer echoes: Observations, theory, and their relationship to noctilucent clouds and subvisible aerosols. J. Geophys. Res., **102**, 2001-2020.

Croskey, C.L., Mitchell, J.D., Friedrich, M., Torkar, K.M., Hoppe, U-P. and Goldberg, R.A. (2001): Electrical structure of PMSE and NLC regions during the DROPPS program. Geophys. Res. Lett., **28**, 1427-1430.

Czechowsky, P., Reid, I.M., Rüster, R. and Schmidt., G. (1989): VHF radar echoes observed in the summer and winter polar mesosphere over Andöya, Norway. J. Geophys. Res., **94**, 5199-5217.

Driscoll, R. and Kennedy, L.A. (1985): A model for the spectrum of passive scalars in an isotropic turbulence field. Phys. Fliuds, **28**, 72-80

Ecklund, W.L. and Balsley, B.B. (1981): Long-term observations of the Arctic mesosphere with the MST radar at Poker Flat, Alaska. J. Geophys. Res., **86**, 7775-7780.

Havnes, O., Brattli, A., Aslaksen, T., Singer, W., Latteck, R., Blix, T., Thrane, E. and Trøim, J. (2001): First common-volume observations of layered plasma structures and polar mesospheric summer echoes by rocket and radar. Geophys. Res. Lett., **28**, 1419-1422.

Hill, R.J.K (1978): Nonneutral and quasi-neutral diffusion of weakly ionized multiconstituent plasma.

J. Geophys. Res., **83**, 989-998.

Holdsworth, D. and Reid, I. (1995): A simple model of atmospheric backscatter: description and application to the full correlation analysis of spaced antenna data. Radio Sci., **30**, 1263-1280.

Hunten, D.M., Turco, R.P. and Toon, O.B. (1981): Smoke and dust particles of meteoric origin in the mesosphere and thermosphere. J. Atmos. Sci., **37**, 1342-1357.

Kelley, M.C., Farley, D.T. and Röttger, J. (1987): The effect of cluster ions on anomalous VHF back-scatter from the summer mesosphere. Geophys. Res. Lett., **14**, 1031-1034.

Khaplanov, M., Gumbel, J., Wilhelm, N. and Witt, G. (1996): Hygrosonde-a direct measurement of water vapor in the stratosphere and mesosphere. Geophys. Res. Lett., **23**, 1645-1648.

Kirkwood, S. and Osepian, A. (1995): Quantitative studies of energetic particle precipitation using incoherent-scatter radar. J. Geomagn. Geoelectr., **47**, 783-799.

Kirkwood, S., Barabash, V., Chilson, P., Réchou, A., Stebel, K., Espy, P., Stegman, J. and Witt, G. (1998): The 1997 PMSE season-its relation to winds, temperature and water vapour. Geophys. Res. Lett., **25**, 1867-1870.

Lübken, F.-J. (1997): Seasonal variation of turbulent energy dissipation rates at high latitudes as determined by *in situ* measurements of neutral density fluctuations. J. Geophys. Res., **102**, 13441-13456.

Lübken, F.-J., Hillert, W., Lehmacher, G. and Zahn, U. von (1993): Experiments revealing small impact of turbulence on the energy budget of the mesosphere and lower thermosphere. J. Geophys. Res., **98**, 20369-20384.

Ratnam, V.M., Rao, D.N., Rao, T.N., Kumar, Y.B., Kumar, V.S. and Rao, P.B. (2002): Coordinated MST radar and Lidar observations for the study of mesospheric strucutes over a tropical station. J. Atmos. Sol. Terr. Phys., **64**, 349-358.

Natanson, G.L. (1960): On the theory of the charging of amicroscopic aerosol particles as a result of capture of gas ions. Sov. Phys. Tech. Phys. (English transl.), **5**, 538-551.

Réchou, A., Barabash, V., Chilson, P., Kirkwood, S., Savitskaia, T. and Stebel, K. (1999): Mountain wave motions determined by the Esrange MST radar. Ann. Geophys., **17**, 957-970.

Summers M.E. and Siskind, D.E. (1999): Surface recombination of O and $H_2$ on meteoric dust as a source of mesospheric water vapor. Geophys. Res. Lett., **26**, 1837-1840.

Thomas, L., Marsh, A.K.P., Wareing, D.P., Astin, I. and Chandra, H. (1996): VHF echoes from the mid-latitude mesosphere and the thermal structure observed by lidar. J. Geophys. Res., **101**, 12867-12877.

*(Received December 18, 2001; Revised manuscript accepted June 7, 2002)*